Accuracy Assessment and Improvement of FMCW Radar-based Vital Signs Monitoring under Practical Scenarios

Accuracy Assessment and Improvement of FMCW Radar-based Vital Signs Monitoring under Practical Scenarios

Brahim Walid
Graduate School of Computer and Information Sciences
Hosei University
Tokyo 184-8584, Japan
walid.brahim.3j@stu.hosei.ac.jp

***Abstract*—Acquisition of human vital signs through radar is a very promising technology that can address the shortcomings of the traditional contact-based measurement devices and enable the move toward a contactless vital monitoring system. This research is focused on monitoring breath rate (BR) and heart rate (HR) via a frequency modulated continuous wave (FMCW) radar. Currently, the two approaches used for BR and HR estimation are filter-based and decomposition-based, such as variational mode decomposition (VMD) for high-quality signal separation. We propose an adaptive VMD (AVMD) to address the problem of setting the number of segmentation levels required by the VMD algorithm. Various experiments are conducted under practical scenarios in terms of distance, angle, posture, and activity as well as the existence of a nearby person and fan. We have made a comprehensive assessment of accuracy change and impact in these scenarios. The experimental results show clearly that the proposed AVMD gives higher accuracy compared to the filter-based and VMD-based. A real-time BR-HR monitoring system using the proposed AVMD and the TI's IWR1843Boost radar board has been implemented to demonstrate its practical uses.**

Keywords—FMCW radar, filter, VMD, AVMD, breathing rate, heart rate, estimation, accuracy, real-time monitoring.

I. INTRODUCTION

Monitoring human heart rate (BR) and breathing rate (HR) is of paramount importance for disease diagnosis, healthcare, and psychological analysis. This is achieved traditionally through special equipment such as ECG (electrocardiogram) monitors, PSG (polysomnography), and wearables like a wristband or watch. However, these approaches suffer from several inconveniences including invasiveness and discomfort due to the need to have direct contact with the human body, which may affect both physical and psychological states. Researchers have tried to address this problem by designing contactless solutions based mainly on cameras [1] and radio frequency signals (RF). Although the former approach using a camera solved the problems of inconvenience and comfort, the privacy is not well preserved specially for continuous monitoring, in addition to the restriction related to light brightness and the line of sight of the camera. On the other hand, RF-based solutions do not have such issues and make them a promising solution for continuously monitoring BR and HR in the background without interfering with human daily activities.

The research on RF-based respiration acquisition was pioneered by J. C. Lin in 1975 [2], and heartbeat detection research was done also by him in 1979 [3]. Due to the availability of highly customized and miniatured radars, the research on using this technology has attracted great attention for both academic and industrial research in the past decade. Different types of radar were used in previous works including Ultra-Wide Band, Continuous Wave (CW), and FMCW radars. In [4], a simple UWB used the Chirp Z Transform (CZT) and a motion filter to recover the respiration and eliminate the motion artifacts. Although the reported results were good, the implementation was not suitable for real-world application. A more recent work using UWB was reported in [5] where a sophisticated system is implemented for continuous monitoring. The breathing was extracted using a bandpass filter and the Short Time Fourier Transform (STFT) was used to extract the heartbeats. They reported a mean absolute error of 0.09 bpm and 1.43 bpm for BR and HR respectively. In [6], a 2.4 GHz CW radar was developed and used to detect the respiratory and cardiac rates of a target sitting at 1.5 cm from the radar. The results obtained were 0.5 bpm and 1 bpm mean average error for the breathing and heartbeats respectively. Using an FMCW radar, the authors in [7] used a combination of VMD and the wavelet transform to estimate the heart rate of a subject sitting at a 1-meter distance. They reported a mean absolute error (MAE) of 0.82 bpm (beats per minute) for the heart rate over a 1-minute window. Wu and Yang used a 5.8 GHz FMCW radar to monitor the heartbeat over one minute with a subject sitting at a 1m distance in a static posture [8]. They used the algorithm of VMD to extract the heartbeat signal and reported an error of 1.7 %. Another recent study also used the VMD decomposition to reconstruct the heartbeat signal from its higher harmonics to avoid the impact of respiration [9]. Their results show that the estimated HR had an MAE in a range of 3.02–6.11 bpm for subjects sitting still at 0.6–0.8 m range. In addition, the use of radar for heart rate monitoring, according to our survey [10] is still lacking and no commercial product is available in the market, due to the unreliability of HR estimations in practical deployment.

Many of the existing RF-based BR/HR studies are conducted under very limited experimental scenarios. It is necessary to evaluate the performance of BR/HR estimation under diverse situations since the radio is very sensitive to both users' and environmental states. Therefore, we conduct a series of experiments to give a comprehensive assessment of BR and HR accuracy under various practical scenarios. We propose the use of an adaptive mechanism for estimating the number of segmentation levels required by the VMD algorithm.

The main contributions of this work are the following: (1) Proposal of adaptive VMD, known as AVMD, that determines the number of the decompositions dynamically

---

Supervisor: Prof. Jianhua Ma

for adaptation to an actual environment; (2) Assessment of both traditional filtered-based and the latest VMD-based approaches as well as our proposed AVMD, which has shown superior performance compared as the former two under practical scenarios; (3) Implementation of a real-time BR-HR monitoring system that can automatically detect human presence and send estimated BR and HR to a user via a network.

The remainder of this paper is organized as follows. The next section describes the general processing chain used for vital sign monitoring. Section III presents details of the proposed AVMD for deciding a proper VMD parameter. The experimental protocols and settings are described in Section IV, and the assessment results are shown in Section V. Section VI explains our developed system for real-time BR and HR monitoring in practical use. The last section gives a summary of this research and a list of issues in future work.

II. Vital Signs Processing

FMCW radar transmits continuous waves that increase in frequency linearly, and this type of wave is called "chirp". Receiving the reflection of these waves from the surrounding environment allows the radar to determine spatial information about the reflecting objects including distance, speed, and angle. In the case of vital signs detection, the radar leverages the change in the range information due to the chest motion resulting from both breathing and heartbeats.

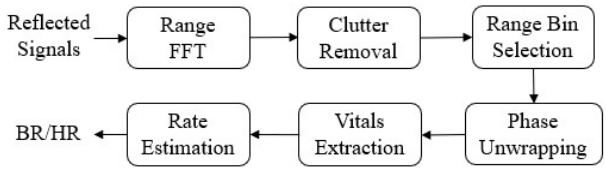

Fig. 1. Signal processing steps radar-based vital sign estimation

The high-level signal processing flow for vitals estimation using radar is depicted in Fig. 1. Upon receiving the reflected radio waves, they are converted into range information by applying a Fast Fourier Transform algorithm (FFT). The output from this step is commonly called 1D-FFT or range-FFT since it provides range information. Clutter removal is applied next to eliminate reflections from static objects in the environment such as the floor, walls, and furniture. This is achieved by subtracting averaged amplitude values in each range bin. Once these static reflections are eliminated, only the manifestation of the non-static chest displacements due to the breathing and heartbeat of a targeted person is expected to have a more significant variable amplitude on the radar range map. The person's chest can be located by just selecting the range bin with the highest average power. Since the displacements of the chest caused by breathing and heartbeats are very minute [11], their impact on the frequency of the reflected signal is very small and cannot be tracked by analyzing the frequency change. However, they can be captured by analyzing the corresponding phase change or demodulation. Due to the restricted output of the phase demodulation process within a range of $[-\pi, \pi]$, a phase unwrapping process is necessary to recover the original evolution of the phase by adding or subtracting 2π value to the phase where consecutive phase values are greater than π. The resulting unwrapped phase signal contains the cardiorespiratory information alongside the target body motion.

To separate and extract the breathing and heartbeat signals, the most reported approach in the literature is based on the use of a band passing filter [12, 13], since the breathing and the heartbeats frequencies are in different ranges. Specifically for a healthy adult human, the breathing and heartbeat rates are 12–20 bpm and 60–100 bpm [14] respectively, which correspond to 0.2–0.33Hz for breathing and 1–1.7 Hz for heartbeats. In addition to this filter-based approach, other popular methods for extraction and separation are based mainly on mode decomposition such as Variational Mode Decomposition (VMD) [15] and Empirical Mode Decomposition (EMD) [16]. They separate the signal into physically meaningful components called Intrinsic Mode Function (IMF). Through spectral analysis of these IMFs, the correct IMF for breathing and heartbeats can be selected based on the frequency range of each signal. This kind of decomposition scheme is specifically suited for analyzing non-linear and non-stationary signals as is the case for breathing and heartbeats. Once the breathing and heartbeat signals are acquired, estimations of their rate change can be performed using a time domain-based approach such as a variation of peak counting algorithm, or through the selection of the frequency of the strongest component in the frequency domain via FFT.

I. Adaptive-VMD-based Vital Signs Monitoring

As mentioned in the previous section, the mode decomposition methods proved their effectiveness for non-linear and non-stationary signal decomposition. Specifically, VMD is reported in the literature [17] to achieve higher precision and noise robustness making it ideal for use in case of vital sign extraction from the noisy reflections in the surrounding environment. Considering better separation results compared to the filter-based one, we adopt VMD as a base for our breathing and heartbeat signal extraction. However, the requirement of providing the number of the decompositions (K) in advance is a major shortcoming of this method since the result of the decomposition is highly sensitive to the value of this parameter and choosing the wrong number will produce sub-optimal and even worse performance. Previous works that used VMD [8, 9, 18] for radar-based vitals extraction provided an empirical value for the parameter K based on their experiments which may not give optimal results in other experimental conditions.

A. Adaptive Estimation of VMD Decomposition Levels

To address the problem of providing the number of decomposition levels, we propose the integration of an estimation scheme to estimate the number of correct decompositions in the context of vital signs extraction. The process is based on the fact that we already know the frequency range of the desired results which is the heartbeat frequency range (0.8-1.7 Hz). To avoid the over-segmentation issue, we start the VMD decomposition with a small value for K (K=3) guaranteeing to have only one valid IMF in the desired range. The next step is to increase the value of K by 1 and check the number of resulting IMFs with center frequency within the heartbeat range. The stop criterion is the generation of more than one valid IMF and in

that case the correct value of K is K-1. We also set a high limit for K to prevent the algorithm from getting stuck in case the decomposition does not yield more than one valid IMF. This process is summarized in Fig. 2.

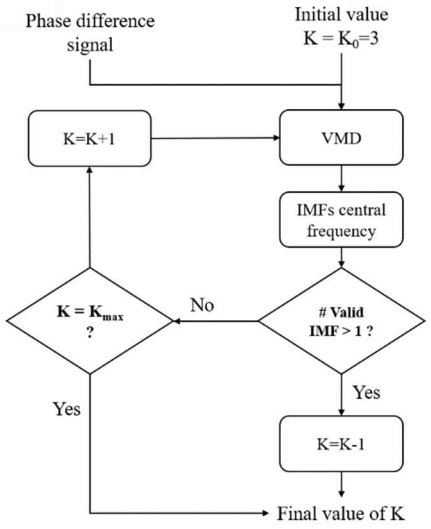

Fig. 2. Flow chart of the process of estimating the number of modes (K)

B. Processing Chain

The processing chain we propose is depicted in Fig. 3. After receiving the range FFT information from the radar, we perform a clutter removal by removing the DC component from the data of each range. We select the target location by choosing the range bin with the highest power. The next step is to apply phase unwrapping to recover the details of the chest displacements. To improve the quality of this data, we perform a phase difference operation, which is specifically applied to amplify the effect of the heartbeat and make it easier for extraction. The breathing signal is extracted next using a bandpass filter with cutoff frequencies of 0.1 to 0.6 last step uses peak counting to estimate the rate of both breathing and heartbeats. The peak counting approach used is the evaluation of the number of peaks in the last 30 sec for breathing and 15 sec for heartbeats. This number is converted into bpm using the following formulas (1).

$$bpm = \frac{60}{estimation\ window} \times number\ of\ peaks \qquad (1)$$

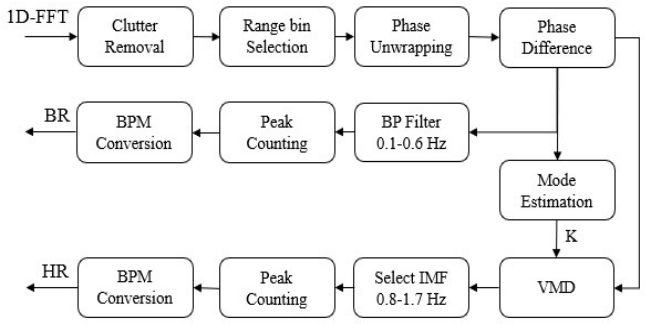

Fig. 3. Flow chart of the vital signs estimation steps.

II. Experimental Setup & Data Acquisition

To validate the performance of our vital sign monitoring approach and assess its robustness for deployment in practical scenarios, we conduct a series of experiments using both an FMCW radar and reference devices under various user and environmental conditions and compare it with the conventional filter-based and VMD-based methods.

A. Devices and Recording Protocol

We adopt the Texas Instrument IWR1843BOOST radar board [19], which is shown on the left of Fig. 4. This radar was selected for its high operating frequency (77 GHz) and bandwidth (4 GHz) in addition to the technical support from Texas Instrument documentation and the online community [20]. We used a modified image file for this board to output the 1D-FFT data through the UART (Universal Asynchronous Receiver/Transmitter) port. The radar settings are given in Table I. To evaluate the accuracy of the estimated BR and HR, we also use two reference devices, the Polar H10 strap [21] and Vernier respiration belt [22], which are shown on the right of Fig. 4.

Fig. 4. Devices: TI-IWR1843BOOST, Polar H10, Vernier respiration belt

TABLE I. Radar Settings

Parameter	Value	Unit
Frequency	77	GHz
Frame periodicity	62.5	ms
Chirp slope	52	MHz/us
Chirp end time	40	us
ADC samples	64	-
ADC sampling Frequency	2	Msps
# Receivers	4	-
# Transmitters	3	-

For this comprehensive assessment, we use a set of python scripts developed in our lab to control the different devices and synchronize the recording. The protocol starts by connecting to the devices (Polar H10, Vernier belt, the radar, and camera) to get the different data. After a successful connection, the software waits for 30 sec before issuing a beep marking the start of the recording. We set the recording time to 3 min where at the end another beep is issued. The software then gathers the data from all devices and writes them into an excel file with each type of data occupying a different sheet, in addition to a video recording for the experiment.

B. Experiment Conditions

In this assessment, our objective is to offer a comprehensive evaluation of the performance of BR and HR estimations using filter-based, VMD-based, and our proposed AVMD. We conducted various experiments that are divided basically into two different categories: user-related and environment-related. The former category is with a subject sitting at different distances, angles, and postures relative to the radar or performing some activity like using a smartphone.

The latter category is related to the surrounding environment such as the impact from a nearby person or other objects placed near the subject. Ten subjects aging from 22 to 31 participated in the different recordings. Each subject recorded one segment of 3 min for each scenario. Table II summarizes the details of the experiments conducted.

TABLE II. EXPERIMENTAL SCENARIOS

Type	Conditions
User	10 participants, distance (0.6, 1, 1.4 m), static, facing radar, 0 deg
	4 participants, angle (0, 25, 50 deg), static, at 1.3 m forming 90deg with radar azimuth axis
	4 participants, posture (facing, back, side), static, at 1.3 m and 0 deg
	2 participants, sleeping (supine, prune, side), radar is 1.2 m on top of the subject's chest.
	2 participants, activity (using a phone), facing radar at 1.3 m and 0 deg
Env	2 participants, a nearby sitting person while the target is facing radar at 1.3 m and 0 deg
	2 participants, moving fan placed next to the target at 1.3 m and -35 deg while the target is at 1.3 m 35 deg.
Long Period	1 participant, 40-min recording of sleep, radar is 1.2 m on top of the subject chest.
	1 participant, 40-min recording while working on a PC. Radar is placed over the PC screen at 1m from the subject's chest

C. Filter-based and VMD-based Processing Chains

Fig. 5 shows the details of the signal processing chains of filter-based and VMD-based methods used for comparison. In addition, for the conventional VMD implementation, we set the parameter K to the value of 10 as it is the default parameter used usually. The first IMF is assigned as the breathing while the second IMF is assigned as the heartbeat.

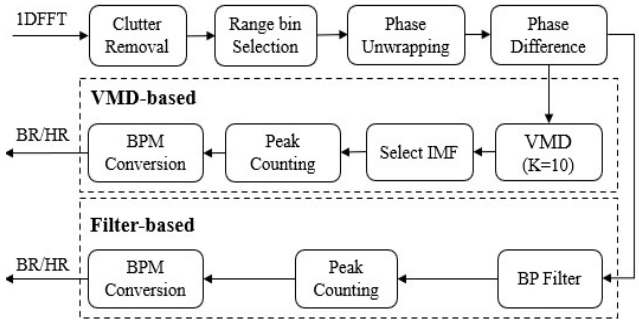

Fig. 5. Filter-based and VMD-based processing chains.

III. ASSESSMENT OF BR AND HR ESTIMATION

In this section, we present and discuss the assessment results based on filter, VMD, and AVMD under various experimental conditions given in Table II of the previous section. The main metric used for evaluation is the Mean Absolute Error (MAE) defined in (2).

$$MAE = \frac{\sum_{i=1}^{n} |Ref_i - Est_i|}{n} \quad (2)$$

where Ref_i is the ground truth value from reference devices, Est_i is the estimated signal value by radar, and n is the total number of values.

A. Impact of Distance

To evaluate the impact of target distance, the subject sits facing the radar at 0.6, 1, and 1.4 m. Table III shows the average MAE for 10 subjects of the estimated BR and HR over 2 min using the three methods. It can be seen that the performance of almost all implementations degrades with increasing distance, especially for heartbeat estimation, which is expected since the signal gets weaker as it travels long distances.

TABLE III. AVERAGE MAE FOR DIFFERENT DISTANCES

Distance (m)	Method	BR	HR
0.6	Filter	1.13	6.29
	VMD	1.76	8.18
	AVMD	1.13	3.04
1	Filter	1.76	7.94
	VMD	3.41	9.59
	AVMD	1.76	4.53
1.4	Filter	1.21	10.58
	VMD	2.35	11.56
	AVMD	1.21	3.59

According to the results from Table III, our adaptive implementation performs better than the conventional Filter and VMD, especially for estimated heart rates.

B. Impact of Angle

We perform recordings at 1.4 meters for angles of 0, 25, and 50 degrees as shown in Figure 6. Four subjects participated in this experiment. Table IV shows a summary of the obtained MAE average results.

Fig. 6. Subject sitting at different angles from radar.

TABLE IV. MAES FOR DIFFERENT ANGLES

Angle (deg)	Method	BR	HR
0	Filter	0.62	10.6
	VMD	0.97	13.8
	AVMD	0.62	3.95
25	Filter	2.07	10.3
	VMD	2.05	10.47
	AVMD	2.07	4.65
50	Filter	1.46	11.93
	VMD	2.54	8.23
	AVMD	1.46	4.56

C. Impact of Posture

To check the accuracy of vital signs estimation in different postures, we perform a recording at 1.4 meters with the subject sitting backward (back to radar) and sideways as shown in Figure 7 and compare it to the previously recorded facing posture. Four subjects participated in this experiment.

Table V shows the obtained average MAE results. The overall results show degradation of performance for all methods for both backward and side sitting. This degradation is understandable since the radar's primary source of reflections related to vital signs is collected from the chest which is obscured in both backward and side sitting. Nevertheless, AVMD still shows better results as compared to the other two methods.

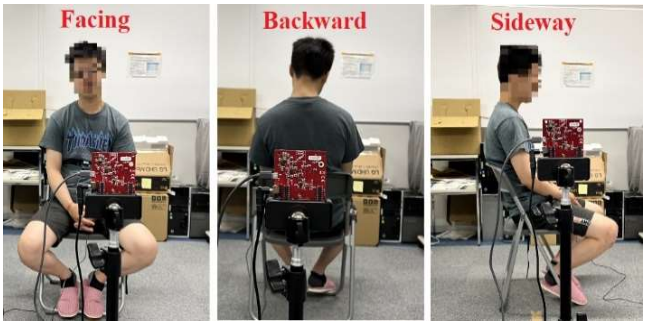

Fig. 7. Subject sitting in facing, backward, and sideways postures.

TABLE V. MAEs FOR POSTURE IMPACT

	Method	BR	HR
Facing	Filter	0.62	10.59
	VMD	0.97	13.87
	AVMD	0.62	3.95
Back	Filter	5.36	15.29
	VMD	7.7	14.48
	AVMD	5.36	11.78
Side	Filter	3.22	8.52
	VMD	2.53	10.15
	AVMD	3.22	5.76

D. *Sleep Scenario*

Different from sitting in a chair, we tested the performance in a sleeping scenario. The postures of supine, prune, and sleeping on the side are considered. Two subjects took part in these experiments with radar placed on top at 1.2 m from the subject's chest. Figure 8 depict the three postures in our experiments.

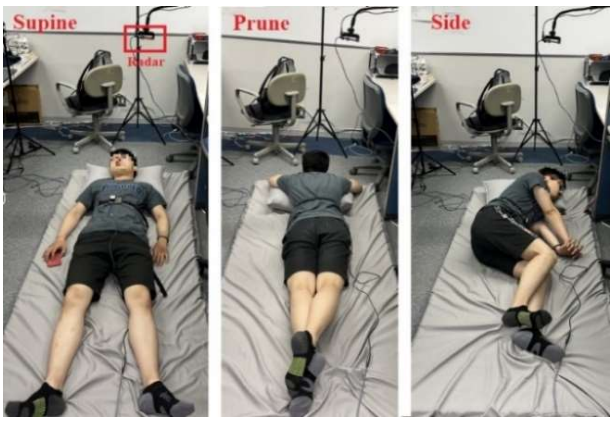

Fig. 8. Subject sleeping in supine, prune, and side postures.

TABLE VI. MAEs FOR POSTURE IMPACT

	Method	BR	HR
Supine	Filter	2.71	10.86
	VMD	3.7	9.7
	AVMD	2.71	3.9
Prune	Filter	2.95	14.57
	VMD	1.96	17.52
	AVMD	2.95	4.7
Side	Filter	2.64	20.39
	VMD	7.4	19.94
	AVMD	2.64	5.6

In both supine and prune postures, AVMD shows very good accuracy for breathing and heartbeat. Specifically in the case of prune, and unlike the previous sitting backward experiment, the presence of the bed mattress pushes back the impact of chest movement that get more visible on the back allowing for better signal extraction result.

E. *Impact of User's Activity*

During this experiment, a subject was sitting on a chair at 1.3 m while using a phone as shown on the left of Fig. 8. Table VI summarizes the MAE results obtained. Even with the subject using his phone AVMD still can get acceptable results from 1.3 m and give better performance compared to the other implementations, especially for HR.

F. *Impact of Other Nearby Subject*

For this experiment, the subject was sitting at 1.3 m while another subject is sitting next to him at a farther range as shown in the right part of Fig. 8. It can be seen, from Table VI, that the performance of estimating the vitals is still within acceptable ranges.

G. *Impact of Other Nearby Objects*

In this experiment, we made use of a moving fan to check the impact on vital estimation accuracy and summarize the result in Table VI. The presence of the fan had some impact that degraded the estimation performance. The AVMD again has outperformed the conventional VMD and the Filter-based methods showing more consistency in estimating the heart rate.

Fig. 9. Subject sleeping in supine, prune, and side postures.

TABLE VII. MAEs OF USING PHONE, NEARBY PERSON, AND FAN

	Using Phone		Nearby Person		Nearby Fan	
	BR	HR	BR	HR	BR	HR
Filter	1.8	16.16	1.18	13.45	3.88	14.16
VMD	5.85	12.8	1.4	7.96	3.86	10.44
AVMD	1.8	5.46	1.18	1.69	3.88	3.78

H. Long Period Experiment

To further test performance in real case scenarios, we recorded additional experiments in sleeping and while working on a PC for 40 min each. For the sleep scenario, the settings are the same as for previous experiments (radar on top at 1.2 m). In the second experiment, the radar was placed over the PC screen using a camera holder where the distance between the radar and the chest of the target is around 1 m as shown in Figure 10.

Fig. 10. Long Period Experiment: sleeping (left), working with PC (right).

Table VIII shows the MAE results for the performance of AVMD where three segments are considered in both experiments.

TABLE VIII. AVERAGE MAES OF AVMD FOR LONG PERIOD MONITORING

	Posture	Time (min)	BR	HR
Sleeping	Supine	0 to 4	0.87	4.08
	Side	4:10 to 13:10	3.47	4.49
	Prune	20 to 30	1.36	2.92
	Avg		1.9	3.83
Working with PC	Facing	0 to 10	3.37	8.15
		15 to 25	4.11	4.34
		30 to 40	2.82	3.82
	Avg		3.43	5.44

The overall results from Table VIII show a slight deterioration in performance in the case working with a PC as compared to the sleeping scenario. This is due to the scattered movements during work as compared with sleep where rare bursts of movements happen. Nevertheless, AVMD still provides very good results for both breathing and heartbeats.

I. Result Discussion

Following the different results obtained from these experiments, AVMD consistently performed better than conventional VMD. The main reason for the unstable performance of the conventional VMD is that the decomposition levels in most cases are not adequate and the IMFs used still have a strong noise impact. AVMD also outperformed the conventional filtering, where the results for the heartbeat extraction were better in all experiments. This is mainly due to the concept behind each method. Whereas the filter will allow any signal components if they are within its cutoff frequencies allowing noises in that range to be aggregated with the signal of the vitals. On the other hand, VMD tries to find the principal components or modes in a signal to separate the noise in the process and result in a higher resolution extraction.

AVMD achieved an average MAE of 4.53 bpm for HR estimation and 1.76 bpm in the case of breathing across distances ranging from 0.6 to 1.4 m in the distance experiments which is the conventional experiment performed by other works. Table IX provides a summary of the performance of AVMD in terms of Mean Absolute Error (MAE) and Mean Absolute Percent Error (MAPE) for each range. According to previous works that assessed the accuracy of wearable measurement devices [24], we define an acceptable error rate for a physical monitoring device to be (< +/-10%), as this is considered an accurate threshold for medical ECG monitors and breathing measurement devices. We use MAPE to compute this error and conclude the accuracy of our solution in the standard sitting scenarios at different distances for 10 subjects (as per previous related works).

TABLE IX. AVERAGE MAES & MAPE FOR DISTANCE EXPERIMENT

Experiment	MAE (bpm)		MAPE (%)	
	BR	HR	BR	HR
Sitting at 0.6 m	1.13	3.04	9.34	4.73
Sitting at 1 m	1.76	4.53	9.58	5.2
Sitting at 1.4 m	1.21	3.59	7.89	5.32

IV. A REAL-TIME MONITORING SYSTEM

This research is further aimed to develop a real-time monitoring system that outputs the estimated BR and HR of a target user. The purpose to develop the system are two folds, one is for researchers to get visualized results to check performance in real-time under various situations, and the other is for a user to be informed in real-time about his/her BR and HR via a smartphone. To this end, we performed different assessments of our proposed processing chain to know the different limitations to expect on deployment. This real-time system has been implemented with the following functions: (1) Acquisition and parsing of the 1D-FFT radar data and measured data from two reference devices, Polar H10 and Vernier belt; (2) Processing the radar data and estimating BR and HR using proposed AVMD to extract the vitals; (3) Desktop GUI of *Development Mode* to connect reference devices for making performance evaluation easier and more direct; (4) Ability to record a video alongside the data from the different the radar and reference devices for easy offline analysis; (5) A mobile App to report the vitals of a target user in real-time via the network.

Python was used as the main development language for the backend implementation, the desktop GUI, and the mobile App. Since multiple tasks need to be executed continuously and in parallel such as reading and parsing radar data from the UART, processing the radar data using the AVMD, managing the GUI, etc. Each of these tasks is started in its independent process using the multiprocessing package to leverage the availability of multi-core CPUs. The communication and data transfer between the different processes are done through data queues available in the same package. To send the processing results to be displayed on the mobile app, we used a MySQL database (DB), so that we can write the vital information (breathing rate and heart rate) into a table inside the DB where the mobile App can issue queries to the server hosting the DB to get the information and display them on the screen of a user's smartphone. Both the desktop

GUI and the mobile App were developed using a library called *Kivy* [23], which is a Python library designed for creating touch-enabled applications. The advantage of using *Kivy* is the use of the same base code with Python and then compiling to other platforms such as Android OS and iOS.

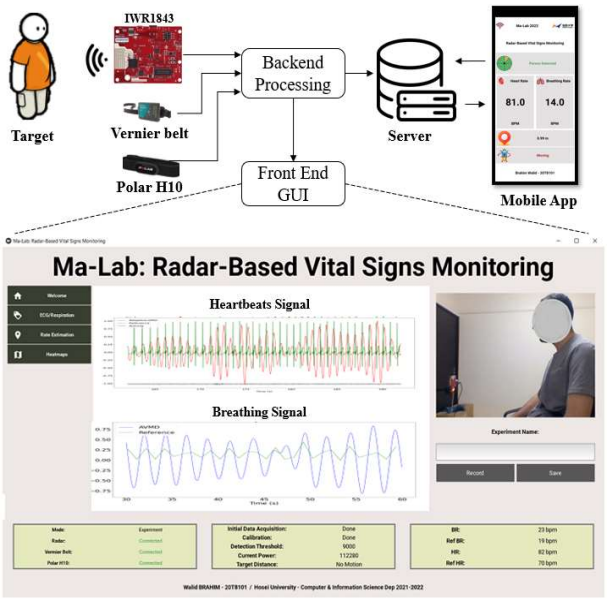

Fig. 11. Vital signs monitoring system components.

The radar captures data at all times, and the vital estimation process will always output an estimation even if there is no person on the scene. To detect the presence of a human, we added a power threshold based on the power level of the room by capturing the data in no-human existence conditions. With the power, if a person enters the scene the power level will rise, and the vital estimation process starts. As soon as the persons exit the scene, the power level will drop, and the vital estimation process stops. The estimation process uses the last 30 sec data as input and proceeds with the same steps as described in our proposal.

V. Conclusion

In this work, we have proposed an adaptive mechanism for estimating the value of the parameter K required by the VMD algorithm used for vital sign extraction and separation. We have given a comprehensive assessment of FMCW radar-based BR and HR estimation accuracy using different methods under various practical scenarios. These assessment results have shown clearly that the proposed AVMD has achieved better and reliable performance compared to the conventional filter-based and VMD-based methods in almost all experiments. A real-time vital sign monitoring system has also been developed to demonstrate its effectiveness for both researchers and users. Our future work will target the acquisition of a more detailed vitals such as RRI and HRV, and using them for more advanced health monitoring such as illness and fatigue. In addition, we will investigate the use of the multiple antennas to enable the monitoring of multiple subjects and extend the capabilities of our platform.

References

[1] N. Molinaro et al., "Contactless vital signs monitoring from videos recorded with digital cameras: an overview", Front. Physiol., Feb 2022.

[2] J. C. Lin, "Noninvasive microwave measurement of respiration", Proceedings of the IEEE, vol. 63, no. 10, pp. 1530-1530, Oct 1975.

[3] J. C. Lin, J. Kiernicki, M. Kiernicki, and P. B. Wollschlaeger, "Microwave apexcardiography", IEEE Transactions on Microwave Theory and Techniques, vol. 27, no. 6, pp. 618-620, Jun. 1979.

[4] A. H. Madsen et al., "Signal processing methods for doppler radar heart rate monitoring", Signal Processing Techniques for Knowledge Extraction and Information Fusion, pp. 121-140, Springer, 2008.

[5] Q. Li, J. Liu, R. Gravina, Y. Li, G. Fortino, "A UWB Radar-based Approach of Detecting Vital Signals", IEEE 17th International Conference on Wearable and Implantable Body Sensor Networks (BSN), pp. 1-4, 2021,

[6] R. Ichapurapu, S. Jain, M. U. Kakade, D. Y. C. Lie, R. E. Banister, "A 2.4GHz non-contact biosensor system for continuous vital-signs monitoring on a single PCB", IEEE 8th International Conference on ASIC, pp. 925-928, 2009.

[7] S. Ma, W. Xue, K. Chen, and Z. Wang, "Radar vital signs detection method based on variational mode decomposition and wavelet transform", China Automation Congress (CAC), pp. 7469-7474, 2021.

[8] K. J. Wu and C. L. Yang, "Heart rate extraction with VMD algorithm in non-stationary clutter environment based on FMCW radar systems", IEEE International Symposium on Radio-Frequency Integration Technology (RFIT), pp. 1-3, 2021.

[9] P. Zheng, C. Zheng, X. Li, H. Chen, A. Wang and Y. Luo, "Second harmonic weighted reconstruction for non-contact monitoring heart rate", IEEE Sensors Journal, vol. 22, no. 6, pp. 5815-5823, 2022.

[10] B. Walid, J. Ma, M. Ma, A. Qi, Y. Luo, Y. Qi, "Recent advances in radar-based sleep monitoring - A review", IEEE Intl Conf DASC/PiCom/CBDCom/CyberSciTech, pp. 759-766, 2021.

[11] A. De Groote et al., "Chest wall motion during tidal breathing", Journal of Applied Physiology, vol. 83, no. 5, pp. 1531-1537, 1997.

[12] S. Iyer et al., "mm-Wave radar-based vital signs monitoring and arrhythmia detection using machine learning", Sensors, vol. 22, no. 9, pp. 3106, Apr 2022.

[13] G. Vinci, T. Lenhard, C. Will, A. Koelpin, "Microwave interferometer radar-based vital sign detection for driver monitoring syst", IEEE MTT-S International Conference on Microwaves for Intelligent Mobility (ICMIM), pp. 1-4, 2015.

[14] "What your heart rate is telling you", Harvard Health Publishing, Aug 30, 2020. Accessed on: Jun. 29, 2022. [Online]. Available: https://www.health.harvard.edu/heart-health/what-your-heart -rate-is-telling-you.

[15] K. Dragomiretskiy and D. Zosso, "Variational mode decomposition", IEEE Transactions on Signal Processing, vol. 62, no. 3, Feb 1, 2014.

[16] S. S. Shen, "Hilbert-Huang transform and its applications", Singapore, World Scientific, 2005.

[17] C. Aneesh, S. Kumar, P.M. Hisham, K.P. Soman, "Performance comparison of variational mode decomposition over empirical wavelet transform for the classification of power quality disturbances using support vector machine", Procedia Computer Science, vol. 46, 2015.

[18] J. Yan, H. Hong, H. Zhao, Y. Li, C. Gu, and X. Zhu, "Through-wall multiple targets vital signs tracking based on VMD algorithm", Sensors, vol. 16, no. 8, pp. 1293, Aug. 2016.

[19] Texas Instruments, "AWR1843BOOST", Accessed on: Aug 14, 2021. [Online]. Available:https://www.ti.com/tool/AWR1843BOOST.

[20] Texas Instruments. "TI support forum", Accessed on: Aug 14, 2021. [Online]. Available: https://e2e.ti.com/.

[21] Polar website. "Polar H10 heart rate sensor", Accessed on: Aug 14, 2021. [Online]. Available: https://www.polar.com/ja/products/accessories/ h10.

[22] Vernier website. "Go direct respiration belt", Accessed on: Aug 14, 2021. [Online]. Available: https://www.vernier.com/product/go-direct-respiration-belt/.

[23] Kivy website. "Kivy", Accessed on: Jun 29, 2022. [Online]. Available: https://kivy.org/#home.

[24] B. W. Nelson, N. B. Allen, "Accuracy of consumer wearable heart rate measurement during an ecologically valid 24-hour period: Intraindividual Validation Study", JMIR Mhealth Uhealth, vol. 7, no. 3, 2019.